Relativistic Electron Dynamics in the Inner Magnetosphere – a Review

R. H. W. Friedel [a], G. D. Reeves [a], T. Obara [b]

[a]Los Alamos National Laboratory, Los Alamos, New Mexico.

[b]Communications Research Laboratory, Koganei-shi, Tokyo, Japan

To appear in JASTP, accepted May 30, 2001
vol 64, issue 2, coverdate January 2002

The dynamics of relativistic electrons in the inner magnetosphere around the time of geomagnetic disturbances have received considerable attention in recent years. In addition to the environmental impact these electrons have on space-hardware in MEO and GEO orbits, and their obvious impact on space weather, the scientific issues surrounding the transport, acceleration and loss of these particles in the inner magnetosphere have not been fully resolved. One of the prime difficulties in understanding the dynamics of relativistic electrons is their somewhat uncorrelated behavior with regard to the major solar wind drivers of the Earth's magnetospheric dynamics (solar wind velocity, density and magnetic field strength/direction) and the major indices representing these dynamics (Dst, Ae, Kp). Relativistic electrons observed at geosynchronous altitude typically reach their peak several days after the onset of a magnetic storm, and a wide range of responses can occur for seemingly similar geomagnetic disturbances. We give here a review and comparison of the current state of research into relativistic electron dynamics, covering simple diffusion, substorm acceleration, ULF wave acceleration and recirculation by ULF waves or plasmaspheric hiss. We present the results of a recent statistical study which has identified the presence of sufficient ULF wave power for a duration of at least 12 hours during a storm as being the most geoeffective indicator of subsequent relativistic electron enhancements at geosynchronous altitudes. For completeness we also briefly examine some of the problems and ideas related to relativistic electron losses.

1. Introduction

There is intense interest in isolating and understanding the mechanisms that contribute to the frequently observed MeV electron flux buildups in the outer magnetosphere, which is frequently observed during the recovery phase of geomagnetic storms.

The interest in these events arises in part because of the increasing evidence of the correlation between the occurrence of these fluxes and of subsequent spacecraft operating anomalies or failures, especially at geosynchronous altitude. The prediction and mitigation of these effects should be possible when the causes of the flux buildups are understood (Baker, 1996). In addition, because of the apparent complexity of these mechanisms, their understanding will contribute significantly to the general knowledge of transport and heating processes in the magnetosphere.

While this is not a new topic, the unprecedented density of observations of relativistic electrons in the inner magnetosphere in the modern era has led to new questions. Data from particle instruments such as on SAMPEX (Baker et al., 1993), POLAR (CEPPAD) (Blake et al., 1995a), GPS (BDD-II) (Feldman et al., 1985), CRRES (MEA) (Vampola et al., 1992), LANL geosynchronous (ESP) (Meier et al., 1996), GOES (Space Systems Loral, 1996), and HEO (Blake et al., 1997) has lead to a revival of relativistic electron research.

Some of the first work in this field was by Williams (1966) who related periodic increases in the trapped relativistic electron populations to increases in the solar wind kinetic energy density.

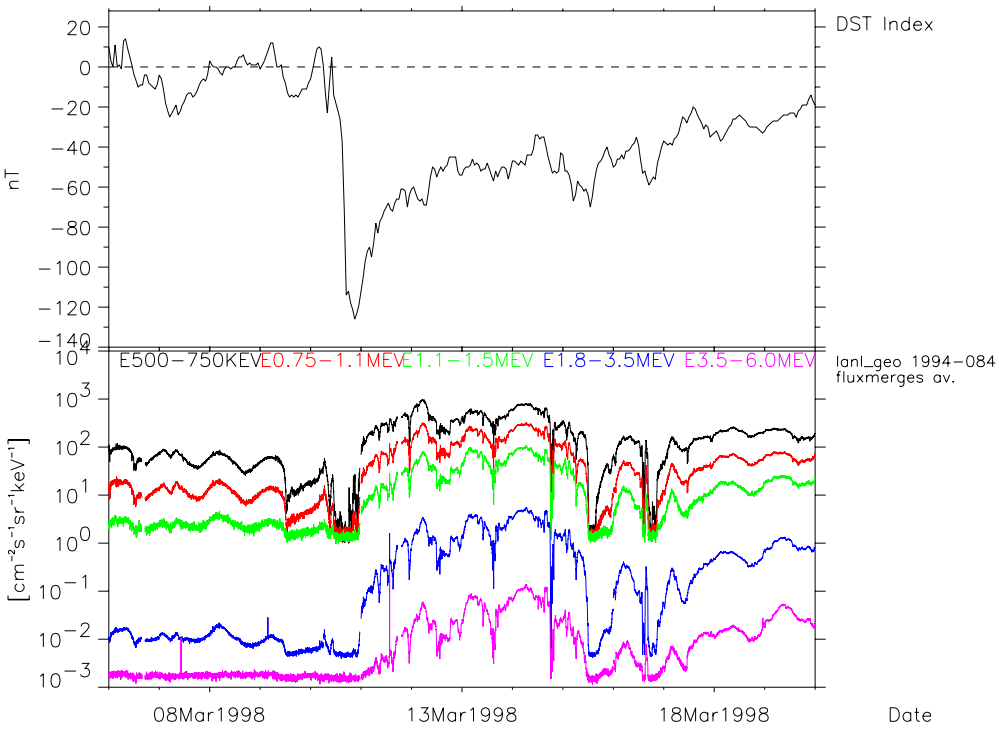

Figure 1. Example of relativistic electron enhancement at geosynchronous orbit following the March 1998 magnetic storm.

Other early work was performed by Paulikas and Blake (1979), who noted the connection between relativistic electron fluxes, magnetic storms and solar wind speed. The most extensive body of observations come from geosynchronous satellites (LANL, GOES). The characteristic and puzzling behavior is shown for example by the March 1998 magnetic storm (Figure 1). A flux dropout is observed during the main phase of the storm, followed by a build up of relativistic electrons to flux levels significantly higher than before the storm. The peak in the response is typically one to three days after the storm main phase, in the middle of the ring current recovery phase. In this example the 1.8–2.5 MeV channel (blue) increases by over two orders (!) of magnitude three days after onset. The delayed response was originally explained by the recirculation model of Fujimoto and Nishida (1990).

Recent, more detailed observations of the storm-time dynamics of relativistic electrons have revealed very fast (< 3 hours) relativistic enhancements deep in the inner magnetosphere which are not consistent with the original recirculation idea, which predicts a much slower rise. This was first noted by Reeves et al. (1998) in a multi-satellite case study of the May, 1997 storm. Figure 2 shows the storm-time dynamics as observed by GPS during that storm. The top panel shows the classical dropout and delayed enhancement near geosynchronous. Further inwards near $L = 5$ the response is more rapid followed by a slight increase over the next few days, while near $L = 4$ the enhancement is rapid, within the time resolution of the GPS orbit (passing through perigee at $L = 4$ every 6 hours). Multiple GPS satellite measurements have shown that this increase at $L = 4$ can occur within three hours or

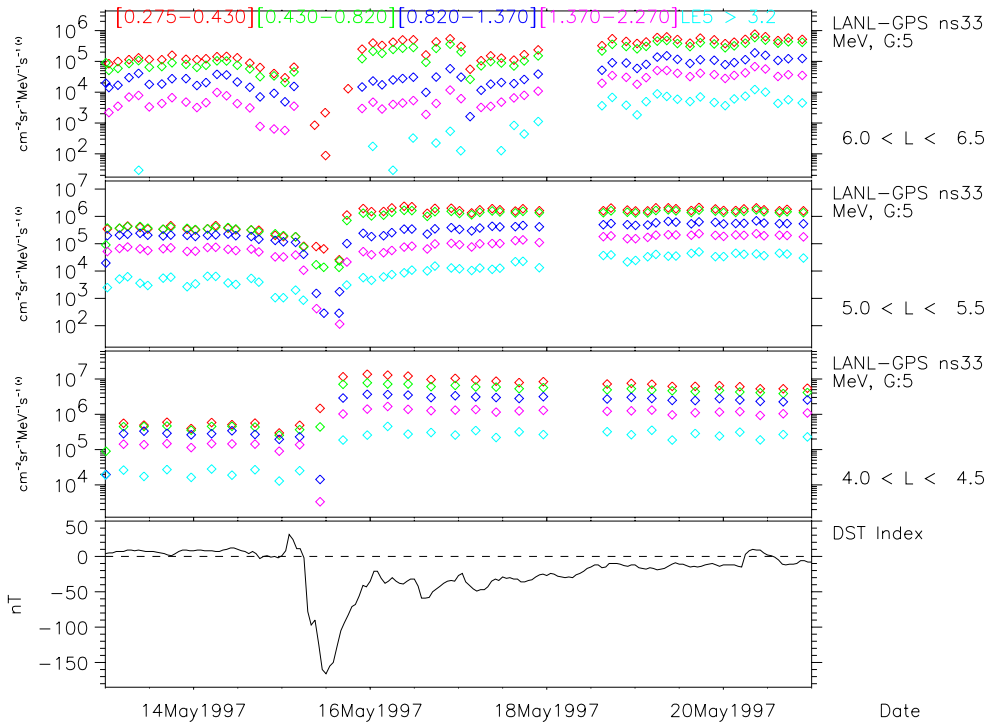

Figure 2. Example of relativistic electron enhancement at various L-values as observed by GPS during the May, 1997 storm.

less (Tom Cayton, private communication).

Another puzzling aspect of these increases has been the range of dynamical responses observed. In a study of the relationship of relativistic electron enhancements at geosynchronous with geomagnetic storms (Reeves, 1998), it was shown that while in general enhancements accompany storms, the magnitude of any given enhancement can vary over a wide range for any given storm strength as measured by Dst. Figure 3 shows the range of relativistic electron enhancements seen at geosynchronous orbit as a function of storm main phase Dst. It seems that for any given storm "strength" (as measured by Dst) a wide range of relativistic electron responses are possible and that the relationship between any controlling input parameters in the solar wind, terrestrial activity indices and the relativistic flux enhancements are not obvious. As one of us has repeat-

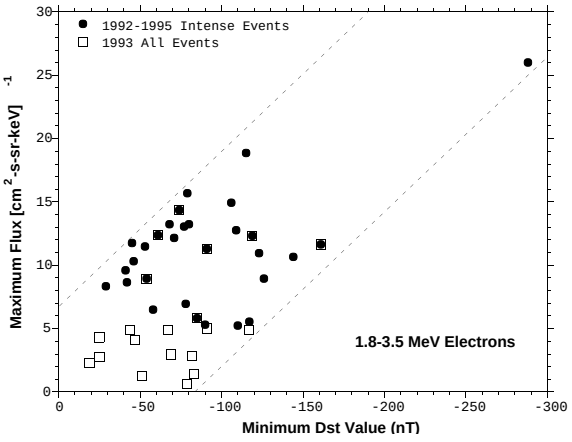

Figure 3. Relationship of relativistic electron enhancements at geosynchronous to strength of storm as measured by Dst, for all storms from 1992 to 1995 (Reeves, 1998).

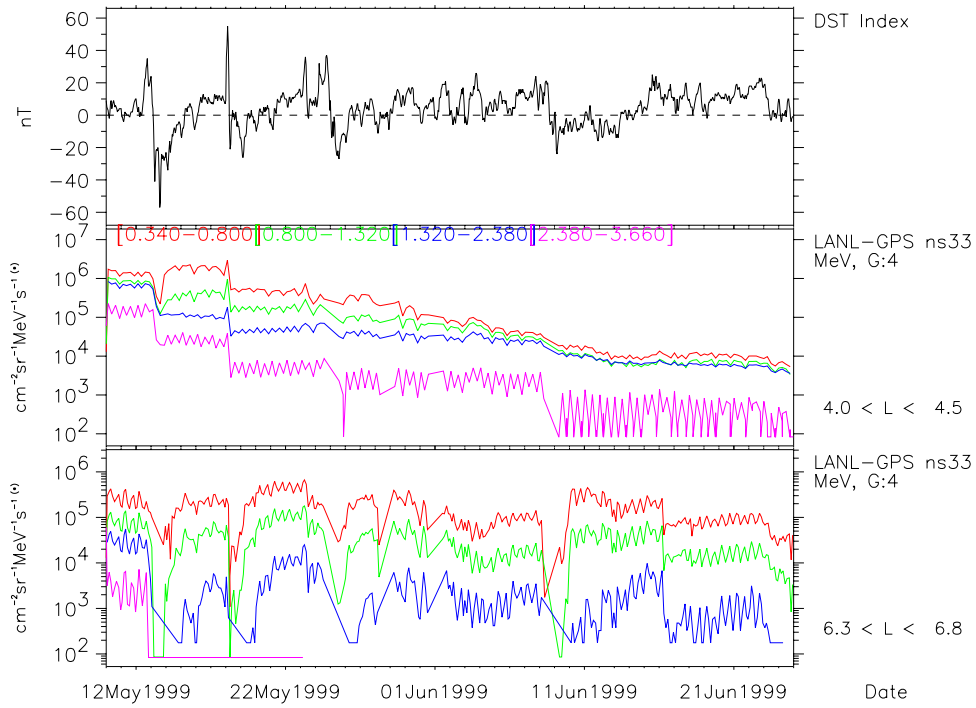

Figure 4. Example of relativistic electron losses in the May to June 1999 period. Shown are Dst (a) and data from GPS NS33 at two cuts through the magnetosphere, (b) near $L = 4.25$, and (c) near geosynchronous.

edly stated, "If you've seen one storm, you've seen one storm!".

While most of the attention has been focused on understanding the flux increase mechanisms, data from the sub-geosynchronous regions has shown many unexplained flux decreases, or "losses". These most commonly occur at storm onset (such as seen in the lower energy channels of Figure 1) but also at other times which may not be related to classical storm onset activity (such as on March 16 in Figure 1). Work by Kanekal et al. (1999) has shown good correlation between measurements in a given L shell between POLAR and SAMPEX in the drift loss cone, which is strong evidence for significant loss into the upper atmosphere. While precipitation may be the predominant loss process at some time here, other processes may be acting at other times, such as magnetopause shadowing (Kistler and Larson, 2000) or adiabatic detrapping in magnetic field inhomogeneities (Imhof et al., 1978). An intriguing example of losses in the inner magnetosphere is given in Figure 4 which shows data from a very quiet period during May to August 1999. The stepwise decreases in the relativistic electron channels measured by GPS near $L = 4$ are very clear. At geosynchronous losses are brief, followed by recovery, while near L=4 the losses are permanent, and fluxes decrease in a stepwise fashion.

The main body of this review is structured into four sections. We first review previous observations of relativistic electron events (Section 2), which has led to the development of several ideas and theories about relativistic electron acceleration in the inner magnetosphere. The most prominent ideas are presented and compared in Section 3. We then look at a body of work that treats these relativistic electron buildup events

in a statistical manner, trying to establish which controlling conditions in the solar wind and/or magnetosphere lead to geoeffective relativistic electron buildups (Section 4). Finally, we will present some recent research into relativistic electron losses (Section 5).

We cannot claim completeness in our approach but hope to present the major observations, proposed mechanisms and statistical studies in the field of relativistic electron dynamics. This is not intended to be an exhaustive review, but rather a report on the status of an ongoing active area of inner magnetospheric research.

2. Observations

As in any field of magnetospheric research, current theories, mechanisms, and models are based on a large volume of observational data. In addition to the studies mentioned elsewhere in the text, we give here a brief and not exhaustive summary of some of the key observations that have influenced current understanding of relativistic electron dynamics.

The earliest extensive observations come from geosynchronous orbit. The first science satellite in geosynchronous orbit was ATS-1 launched in 1966. Paulikas and Blake (1971) compiled a detailed report on some of the early work on the particle environment at synchronous orbit. Baker et al. (1988) and Cayton et al. (1989) presented further comprehensive measurements of relativistic electrons at geosynchronous orbit based on the Los Alamos geosynchronous measurements. Based on these data Baker et al. (1989) found relativistic electron butterfly pitch angle distributions observed near geosynchronous local noon and speculated that these are consistent with the Nishida (1976a) recirculation process.

In the 1990s the advent of multi-satellite event analysis and the shock injection of the March 24, 1991, storm was instrumental in causing a resurgence of community interest in relativistic electrons. This event has been well modeled (Li et al., 1993; Hudson et al., 1997), but this type of event is comparatively rare. Extensive work on shock acceleration has been also been done for the great storm of January 10, 1997 (Li et al., 1998b).

There have been several other case studies that also investigated the relativistic electron response during storms: The US National Space Weather event, the November 1993 storm (Li et al., 1997a; Knipp et al., 1998), and the US NSF (National Science Foundation) GEM (Geospace Environmental Modeling) storms of May 1997 (Li et al., 1999) and January 1997 (Selesnick and Blake, 1998; Reeves et al., 1998). The event-driven studies of the GEM inner magnetosphere storms campaign in particular where instrumental in bringing together observations and theory from a broad spectrum of magnetospheric researchers to address the problem of the relativistic electron dynamics.

Further work on the dynamics of relativistic electrons was performed by Baker et al. (1994) and Nakamura et al. (1998) who used SAMPEX data to characterize the storm-associated relativistic electron acceleration and decay times in the inner and outer radiation belts. While the decay times were found to be consistent with slow pitch angle diffusion and loss into the atmosphere (5–10 days), the rise times (1–2 days) led the authors to suggest that "the Earth's magnetosphere is a cosmic electron accelerator of substantial strength and efficiency."

In a further examination of SAMPEX data Nakamura et al. (1995) and Blake et al. (1995b) reported short, intense relativistic electron precipitation bursts at storm onset and argued for the presence of a strong scattering process. This has been investigated in more detail by Nakamura et al. (2000); Lorentzen et al. (2001) and Blake et al. (2001).

While most of the previous authors noted an association of solar wind velocity enhancements with relaltivisitic electron enhancements, Baker (1996) performed a more detailed correlation study of outer zone relativistic electron changes with upstream solar wind and magnetic field features, which yielded a southward B_Z (or stormtime) dependence and a good correlation with solar wind speed. This idea was expanded when Baker et al. (1997) examined relativistic electron enhancements associated with recurrent geomagnetic storms, which indicated that high-speed solar wind streams are geoeffective in producing re-

laltivisitic electron enhancements. Obara et al. (1998) investigated the effects of the interplanetary magnetic field on the enhancement of relativistic electrons during the storm recovery phase and confirmed the results of Baker et al. (1997).

Fung and Tan (1998) analyzed the low altitude trapped relativistic electron data from the Japanese OHZORA satellite during magnetic storms and correlated them with solar wind speeds. The 2.5-day, 13-day, 27-day and 54-day correlation peaks previously reported for energetic electrons near geosynchronous orbits are also clearly seen, suggesting a good coherence between relativistic electron measurements at different regions in the magnetosphere.

Rostoker et al. (1998) identified a close and consistent association between large-scale ULF pulsations and the intensification of relativistic electron flux at geostationary orbit and speculated that ULF waves may play a significant role in accelerating electrons to relativistic energies. They also noted that ULF waves tend to accompany high speed solar wind streams.

Baker et al. (1998b,a) suggested that relativistic electron production requires two ingredients: a "seed" population of 100–200 keV electrons in the outer magnetosphere and a long-duration, powerful occurrence of ULF waves in the PC4–5 frequency range. The former was to be supplied by substorms during the main phase of the storm, while the latter would then "pump up" the electrons to relativistic energies. The requirement of a "seed" population received further support in a case studies of the May 2, 1998 storm (Obara et al., 2000a; Blake et al., 2001) and the November 1993 storm (Obara et al., 2000b).

In a further search of "classes" of storms that led to relativistic electron enhancements, Kanekal et al. (2000) examined the relativistic electron response for the class of magnetic storms caused by magnetic clouds in 1997 and noted that enhancements tend to occur over a broad range of L-values suggesting a global nature of the underlying acceleration mechanism.

Studies which treat the relativistic electron dynamics from a more statistical point of view are covered in Section 4.

3. Relativistic electron buildup

Relativistic electron enhancements can be separated into three general "classes" of events. All are associated with magnetic storms:

A. Shock acceleration. These are associated with very large magnetic storms but are comparatively rare. While Li et al. (1993) was able to model in detail the great shock event of March 24, 1991, this remains a unique event. In spite of a wealth of ISTP observations of the effects of shocks impinging upon the magnetosphere, no such creation of a new radiation belt has since been observed. There remain several unanswered questions here as to what conditions are required for the shock mechanism to overwhelm all other energetic electron processes; this, however, does not fall within the scope of this review.

B. Slow buildup. These are the events first studied, and are the generally considered to be the "typical" response to high speed solar wind streams (Baker, 1996).

C. Rapid buildup. These enhancements occur in relation to many magnetic storms. These dynamics are common, but are as yet not fully understood.

Consistent with the complexity observed in the dynamic behavior of common relativistic electron buildup, several candidate mechanisms have been proposed for both the fast and delayed buildup of the MeV electrons in the magnetosphere:

1. Large scale recirculation in the magnetosphere involving radial diffusion and pitch angle scattering (Fujimoto and Nishida, 1990);

2. Jovian electrons as a source for MeV electrons in the magnetosphere during those times when the interplanetary magnetic field lines connect Jupiter and Earth (Baker et al., 1979, 1986);

3. small scale recirculation in the magnetosphere involving radial diffusion and pitch angle scattering (Boscher et al., 2000; Liu et al., 1999);

4. electron cyclotron heating by whistler waves (Temerin et al., 1994; Li et al., 1997a; Summers et al., 1998);

5. adiabatic effects in a storm recovery as the earthward motion of flux surfaces during the Dst decay energizes electrons and ions (Kim and Chan, 1997; McAdams and Reeves, 2001);

6. enhanced radial transport through interaction with ULF pulsations, which leads to inward transport and adiabatic heating of electrons whose drift frequency satisfies a resonance condition with the pulsation frequency (Hudson et al., 1999; Elkington et al., 1999);

7. diffusion of trapped energetic electrons in the cusp into the radiation belts (Sheldon et al., 1998);

8. enhanced earthward transport from $x \approx -10R_E$ to geosynchronous altitude of MeV electrons by direct substorm injection (Ingraham et al., 1999, 2000, 2001)

9. and by enhanced radial diffusion alone (Hilmer et al., 2000; McAdams et al., 2001). Here the diffusion mechanism is left unspecified, but the authors argue that on the basis of the phase space density gradients observed radial diffusion alone (no recirculation) could account for the observed flux increases.

These mechanisms fall broadly into two categories. Those which rely on an increased source population and/or radial transport only (2, 5, 8, 9), and those which propose a magnetospheric "source" or internal acceleration mechanism (1, 3, 4, 6). We examine each of these proposed mechanisms in turn below.

3.1. Large scale recirculation

Fujimoto and Nishida (1990) applied the recirculation model that was originally proposed for trapped energetic electrons in the Jovian magnetosphere (Nishida, 1976a) to energetic electrons in the earth's magnetosphere. The main feature of this model was to combine conventional radial diffusion with the essentially energy preserving cross-L diffusion at low altitudes. The schematic of the proposed model is presented in Figure 5. Sentman et al. (1975) added pitch angle scattering near the equator to this process, thereby providing an added mechanism to move electrons to lower altitudes along a field line. They suggested

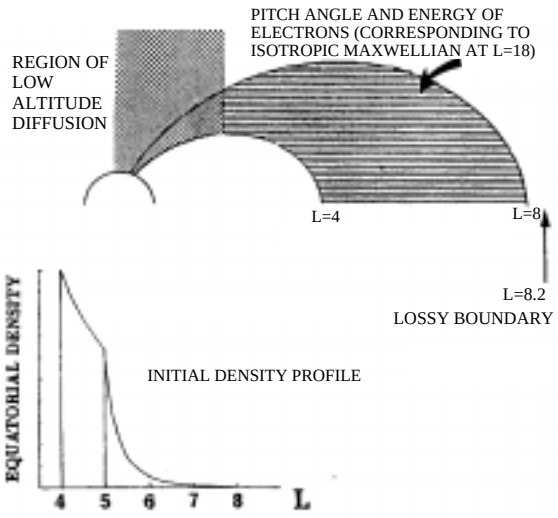

Figure 5. The model Earth magnetosphere used in the recirculation model of Fujimoto and Nishida (1990).

that some particles could reach very high energies by going through this process repeatedly. The idea of particle acceleration by multimodal diffusion had been proposed before by several authors (Roederer, 1970; Schulz and Lanzerotti, 1974).

The main problem with this recirculation model is the low-altitude cross-L diffusion part of the recirculation loop. Fujimoto and Nishida (1990) refer to "ULF turbulence observed in the high latitude ionosphere" as being potentially responsible for this diffusion. At low altitude and high magnetic field strengths cross–L diffusion by any mechanism is difficult as particles are very rigidly guided by the magnetic field and ULF waves at low L are less than 0.1% of the ambient magnetic field strength. Scattering can occur by interaction with the neutral atmosphere near the mirror points, but this process leads more to loss than cross–L diffusion. In the model the low altitude diffusion is needed as the magnetic field strength remains virtually constant across small variations in L, allowing for constant energy diffusion while effectively moving the electron radially out at the equator. Furthermore, the recirculation loop is slow (as it involves radial transport over several R_E); consequently, while this adequately explains the delayed flux enhancements

seen at geosynchronous orbit (Figure 1) and is the main strength of the model, it does not explain the more recently observed rapid enhancements at lower L (Reeves et al., 1998) (Figure 2).

3.2. Jovian electron source

Nishida (1976b) showed that trapped energetic particles from the Jovian radiation belts can at times undergo enhanced outward diffusion and leak into the interplanetary medium. Baker et al. (1979, 1986) then proposed that, during times when the Earth and Jupiter are on the same branch of the interplanetary magnetic field (Parker spiral), these Jovian electrons can enter the terrestrial magnetosphere and could form a source of the observed relativistic electron population. While this may explain the presence of relativistic electrons in the Earth's magnetosphere, it cannot explain the storm-time dynamics; after all, geomagnetic storms occur independent of any Earth-Jupiter "connectivity". While there is evidence that Jovian electrons can be observed on the open magnetic field lines of the polar cap (Figure 6 (Kanekal et al., 1998)), the contribution to the trapped fluxes in the main body of the radiation belt is negligible. Figure 6 shows the relativistic electron fluxes observed in the solar wind, showing clear cyclical increases associated with the times of interplanetary magnetic field connection with Jupiter. The same variation can be observed in the Earth's polar caps. However, the level of flux is very low, and this association disappears in the inner magnetosphere.

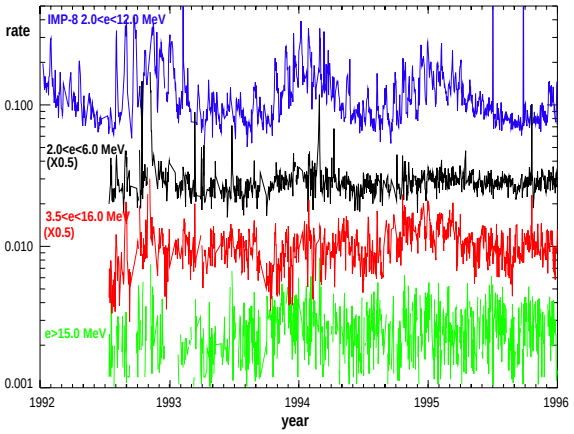

Figure 6. SAMPEX measurements of relativistic electron rates in the polar cap $L > 10$, together with relativistic electron data in the solar wind from IMP-8.

3.3. Small scale recirculation

The original recirculation model by Fujimoto and Nishida (1990) cannot explain the rapid flux enhancements observed near $L = 4$. Work by (Boscher et al., 2000; Liu et al., 1999; Summers and Ma, 2000) has taken the recirculation idea further and applied it on a smaller spatial scale. This is based on the recognition that in the simultaneous presence of both pitch angle and radial bi-directional diffusion there will always be a path for some electrons to gain energy. The differences in the various approaches are the physical mechanisms that lead to radial and pitch angle diffusion.

3.3.1. The Salammbô model

In the Salammbô diffusive radiation belt code (Beutier and Boscher, 1995; Bourdarie et al., 1996; Boscher et al., 2000) radial diffusion is modeled by activity-dependent electric and magnetic field fluctuations, while pitch angle diffusion is modeled by wave-particle interactions with hiss near the plasmapause. Figure 7 attempts to illustrate the recirculation process in a schematic manner. Diffusion is relatively fast and predominates beyond $L = 4$. Inward of $L = 4$ diffusion is relatively slow and pitch angle diffusion predominates, leading to electron precipitation and loss. At the boundary where both processes are comparable, electrons can undergo many cycles of coupled radial and pitch angle diffusion: Inward radial diffusion is followed by pitch angle scattering to lower pitch angles, outward radial diffusion at higher latitudes and subsequent pitch angle scattering to higher pitch angles. While both scattering processes have a preferred directionality they are bi-directional processes, so that a given fraction of electrons undergo this cycle. Energy gain occurs because the pitch angle scattering process tends to preserve energy (momentum scattering

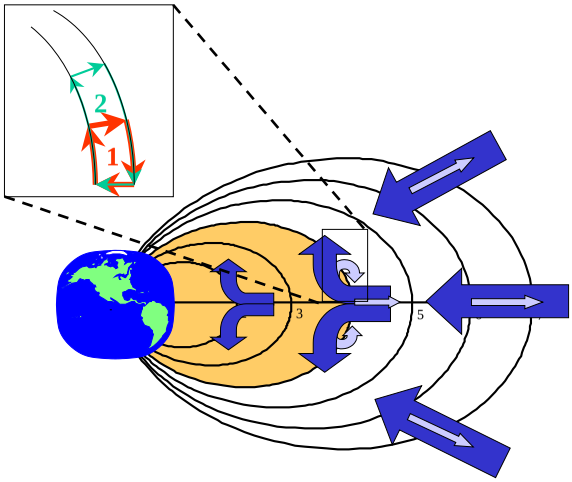

Figure 7. Schematic of radial and pitch angle diffusion processes and their directionality and relative strengths.

only) while the electrons gains more energy due to adiabatic heating on inward radial transport at the equator than it loses on outward transport at higher latitudes.

In this way an electron can undergo many small recirculation loops locally, which can explain the rapid build-up of relativistic electrons near $L = 4$, while the subsequent delayed increase at geosynchronous is explained by the outward diffusion time scales. Figure 8 shows the Phase Space density (PSD) profiles predicted by the code as a function of μ which shows a clear PSD peak near L=4.

A detailed comparison of Salammbô model performance with GPS in-situ measurements is shown in Figure 9. The Salammbô code is run with LANL geosynchronous data as boundary condition (electrons up to several hundred keV) and Kp as input, which parameterizes radial diffusion strength and plasmapause position. Figure 9 compares the model outputs at 1.5 MeV and 400 keV to the radial cuts measured by GPS in the same energy range. Since the code does not include losses due to dropouts, it is started from a quiet, stationary state. Both energy ranges are well reproduced in the code, the relativistic electron channel showing the rapid enhancement at $L = 4$ and the slower, delayed increase at higher L-values.

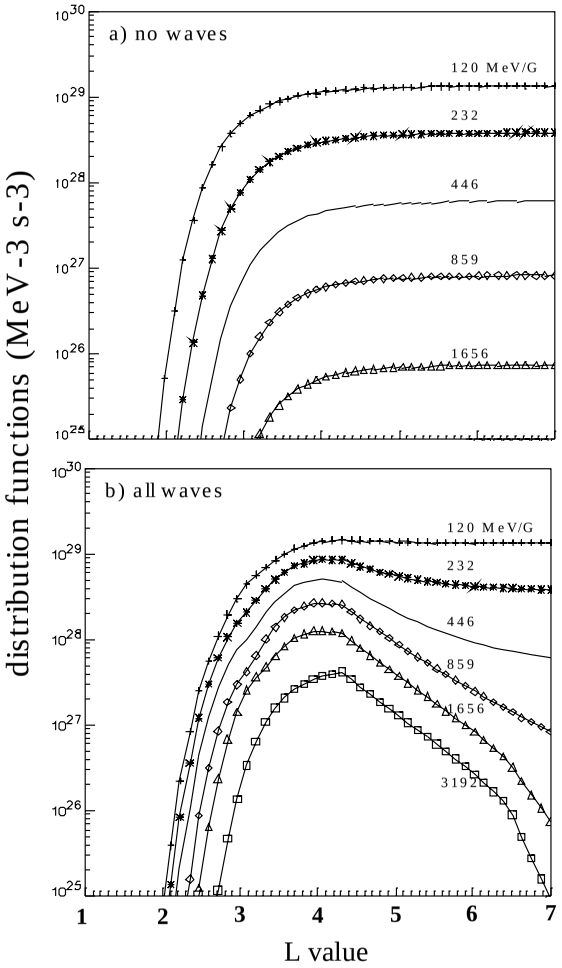

Figure 8. Salammbô predictions of phase space density profiles for the case of a) no waves and b) with waves

3.3.2. Magnetic pumping by ULF waves

Liu et al. (1999) presented a detailed theoretical study of an internal acceleration mechanism by large scale ULF waves, to explain the observations of Rostoker et al. (1998). This new magnetic pumping mechanism seeks to "speed up" by replacing the slow radial diffusion steps of the Fujimoto and Nishida (1990) recirculation model with faster means to achieve global recirculation. Using global ULF waves as an alternate transport mechanism, the slow, meandering of radial diffusion (taking days) is replaced by the fast, convective $\mathbf{E} \times \mathbf{B}$ drift which accelerates the recirculation cycle to the timescale of the waves (minutes).

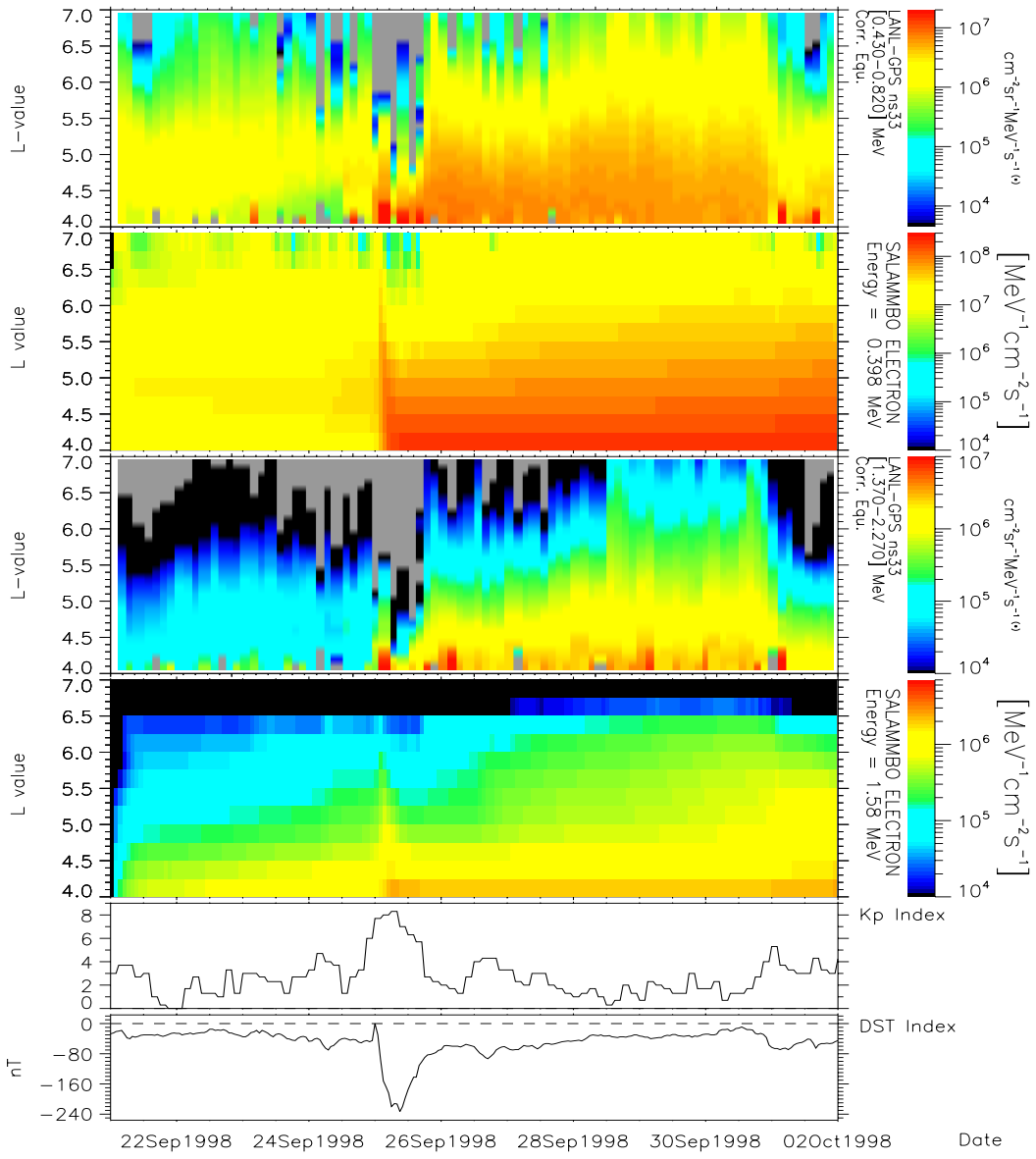

Figure 9. Salammbô run for the September 1998 storm.

Furthermore, there is no need for an exclusive cross-L displacement at low altitudes (Fujimoto and Nishida, 1990), as ULF waves will recycle particles at at all points along a field line; the large scale recirculation is replaced by the sum of many small recirculation loops.

From indirect estimates Liu et al. (1999) show that with a reasonable choice of ULF wave amplitude, a flux level of $10^3 \mathrm{cm}^{-2}\mathrm{s}{-}1\mathrm{sr}^{-1}$ for > 1 MeV electrons can be generated at geostationary orbit in a time frame of 2.4 to 5.3 hours.

This theory is still at the developmental stage, mainly because of the over-simplified treatment of pitch angle diffusion as a homogeneous process independent of space, energy, and pitch angle.

3.3.3. Electron cyclotron heating

The basic concept of energy diffusion of relativistic electrons resulting from resonant interactions with whistler mode waves in the magnetosphere was originally discussed by Temerin et al. (1994) and Li et al. (1997a). Horne and Thorne (1998) identified potential wave modes that are capable of being in resonance with the important electron energy range of 100 keV to a few MeV. The principal waves are L mode electromagnetic ion cyclotron (EMIC) waves, oblique magnetosonic waves, and R mode whistlers.

Work by Summers et al. (1998) included this concept in their proposed model. This model is based on diffusion coefficients for gyroresonant electron-whistler mode wave interaction, a source representing substorm-produced (lower-energy) seed electrons, and a loss term representing electron precipitation due to pitch angle scattering by whistler mode and EMIC waves.

Figure 10 gives a schematic description of the regions where enhanced levels of both EMIC and whistler mode chorus occur during a storm. In this picture, the wave activity can account for both the loss and subsequent acceleration of relativistic electrons.

Intense EMIC waves are excited near the dusk-side plasmapause (as a result of cyclotron resonance with anisotropic ring current H^+ ions). These waves can cause rapid pitch angle scattering of trapped $\gtrsim 1$ MeV electrons, which can contribute to the main phase depletion of these electrons throughout the outer zone. Even though the scattering region is limited, loss times in the order of hours can be obtained. Observational evidence (Lorentzen et al., 2001) shows a clear preference of precipitating microburst near dawn as observed by SAMPEX; which could be related to the chorus location in Figure 10.

Chorus emissions can be excited by substorm activity during the storm recovery, which can also maintain modest levels of EMIC waves. Electrons in the outer zone can interact with both types of waves, which in turn leads to diffusion in pitch angle and energy, leading to a process of stochastic acceleration (Summers and Ma, 2000).

In the model calculation performed by Summers and Ma (2000), assuming reasonable parameters for whistler mode waves, background plasma density and other model parameters, they obtained the observed high-energy steady state distributions on the timescale of 3–5 days. The gradual acceleration process formulated by Summers and Ma (2000) is not intended to apply to major storms which produce enhancements on the order of hours. However, this mechanisms may well be particularly effective for small, moderate magnetic storms with long recovery phases that have plenty of substorms.

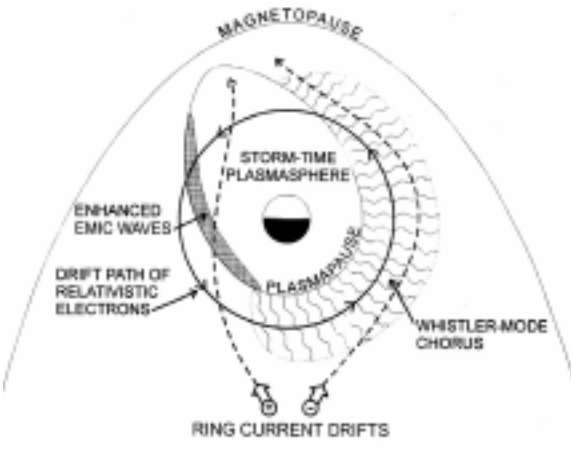

Figure 10. Schematic diagram showing spatial distribution of whistler mode chorus and EMIC waves during magnetic storms in relation to the position of the plasmapause and the drift paths of ring current ($10 - 100$ keV) electrons and ions an relativistic (~ 1 MeV) electrons. This map is taken from Summers et al. (1998); the regions of wave activity are determined empirically from published data.

Other theoretical work (Roth et al., 1999) extends the theory of Summers and Ma (2000) to include whistler waves propagating obliquely to the magnetic field. If the wave is traveling only parallel to the magnetic field, only the lowest order resonant interactions (cyclotron and Landau) produce changes in electron pitch angle and energy. Oblique propagation enables higher order resonant interactions whenever the Doppler shifted wave frequency equals any integer multiple of the local gyrofrequency. For relativistic electrons moving along an inhomogeneous mag-

netic field there exist typically several harmonic interactions, and since the gyroradius of the electron may be of the order or greater than the perpendicular wavelength, the strength of the interaction at the higher harmonics is of the same order as at the fundamental. The simulations performed by Roth et al. (1999) indicated that this process alone may contribute to a 10–100 fold increase in the relaltivisitic electron flux in the outer radiation belt, at time scales of 30-60 min, sufficient to also explain the observations of fast relativistic electron enhancements.

Both these whistler wave related processes depend on substorm injections of a 10-100 keV "seed" population, which act both as seed for subsequent acceleration and lead to an increase in whistler wave intensity. This forms an interesting link between substorm generated waves and enhancements of relativistic electrons during geomagnetic storms and other active periods.

3.4. Dst effect

During the course of a magnetic storm the ring current increases drastically due to the trapping of fresh plasma-sheet material in the inner magnetosphere (Williams, 1987; Korth et al., 2000). The ring current then decays at a slower rate. The Dst index is a proxy for this process. The ring current itself induces an magnetic field that adds to the Earth's ambient field. It is this induced change that can affect the flux levels of energetic particles at a given location, as they will rearrange themselves in order to preserve their third adiabatic invariant. This can lead to local increases or decreases of the observed particle population (Kim and Chan, 1997). This is an adiabatic process which does not lead to a net energy gain or loss, but it is mentioned here for completeness as it might have the appearance of an energy gain or loss. In studying the response of relativistic electrons during storms this effect has to be taken into account and "subtracted out" to reveal the true dynamics. Figure 11 shows the effect of this for data from the November 2, 1995 storm. This shows that the corrections due to Dst are largest around onset, leading to a *smaller* actual flux dropout that suggested by the uncorrected data. McAdams and Reeves (2001) also

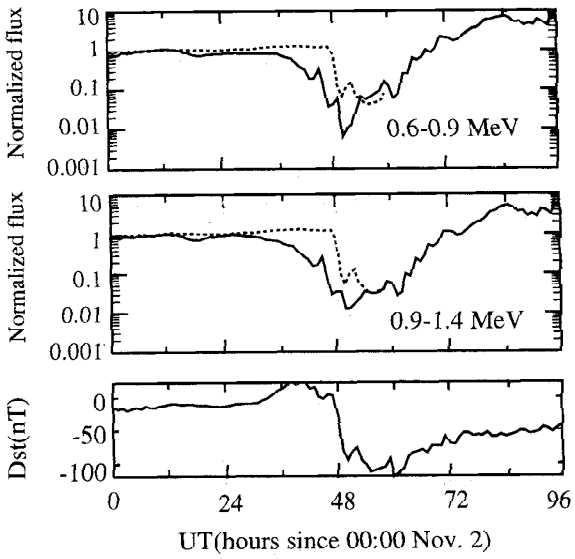

Figure 11. LANL geosynchronous data for two energy ranges 0.6–0.9 and 0.9–1.4 MeV) for the November 2, 1995 storm. Solid lines are actual data, dashed line data corrected for Dst according to the Ding-Toffoletto-Hill field model. From Kim and Chan (1997).

incorporated the Kim and Chan (1997) Dst correction into their work and showed that there is a residual net flux increase of relativistic electrons when the Dst effect has been subtracted.

3.5. Direct heating by ULF

The observed association of ULF waves and relativistic electron enhancements (Baker et al., 1998b,a; Rostoker et al., 1998) have also led to an alternate approach to Liu et al. (1999) in explaining the role of ULF waves in relativistic electron enhancements.

In MHD/particle simulations of the January 1997 event Hudson et al. (2000, 1999), inward radial transport and adiabatic acceleration of outer zone electrons was compared with *in situ* observations over a period of several hours. Following the observation of large-amplitude, near-monochromatic ULF oscillations in the H component of the magnetic fields at College and Gakona, Alaska during this period, a spectral analysis of the MHD fields used to drive the simulations was undertaken. The mode struc-

ture obtained in this analysis led to the proposal that electrons could be adiabatically accelerated through a drift-resonance via interaction with toroidal-mode ULF waves (Hudson et al., 1999). This is a rare case of modeling work leading to the proposal of a new physical mechanism.

Elkington et al. (1999) performed a quantitative investigation into the nature of such drift-resonant acceleration, by tracking particle trajectories in a simplified field model consisting of a compressed dipole and global, toroidal-mode Pc-5 ULF waves. In such an asymmetric magnetic field, a particle with drift frequency ω_d satisfying $(m \pm 1)\omega_d - \omega = 0$ will gain energy through drift-resonant interaction with toroidal-mode waves of frequency ω and global mode number m. Their proposed acceleration mechanism is illustrated in Figure 12. In this example, an equatorially-

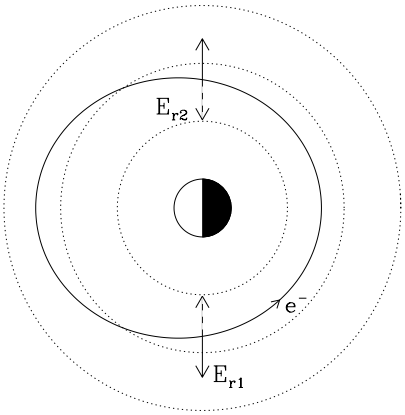

Figure 12. Electron drift path (compressed dipole) with electric fields indicated for an m=2 mode. Solid arrows indicate the electric field at t=0 for an electron starting at dusk, while the dashed arrows indicate the electric field direction half a drift period later (Elkington et al., 1999).

mirroring electron in a compressed dipole interacts with a global m=2 toroidal-mode wave of frequency ω. At t=0 the electric fields are indicated by the solid arrows. An electron starting at dusk and moving with a drift frequency $\omega_d = \omega$ would first see a positive radial electric field while undergoing negative radial motion and half a drift period later a negative electric field while moving radially outward (dashed arrows). The resulting product $E_r dr$ is therefore negative over the orbit of the electron, leading to a net energy increase.

The addition of a convection electric field to this process is what makes it possible to accelerate particles in bulk using resonance with toroidal waves. Without the effect of the convection fields, particles on one side of the resonance would gain energy while particles on the other side of the resonance would lose energy, resulting in a bulk acceleration limited to that arising from energy asymmetries in the resonant island. The addition of the convection electric field makes it possible to accelerate particles regardless of their initial phase. In principle it is possible to adiabatically accelerate electrons with 10-100 keV energies at the magnetopause to MeV energies in the inner magnetosphere, using drift-resonant acceleration and a strong convection electric field. For example, an electron with an initial energy of 80 keV at 10 R_E at local noon would have an energy around 200 keV at geosynchronous, and exceeding 1.1 MeV at 3 R_E (Elkington et al., 1999).

The results of a sample simulation are shown in Figure 13 which shows the average particle energy in (b),where it is clear that there has been bulk energization, while (a) shows the later phase bunching, resulting from the effect of radial electric fields on the azimuthal drift velocity of particles.

3.6. Substorm acceleration

Substorms are generally associated with the injection of electrons of energy up to only a few hundred keV (Cayton et al., 1989; Baker et al., 1989). Successful modeling of an electron substorm injection up to a few hundred keV has been done (Birn et al., 1998; Li et al., 1998a; Zaharia et al., 2000).

Ingraham et al. (1996, 2001) give evidence that strong, repetitive substorms (such as occurred in the recovery of the March 24, 1991, storm) can directly transport MeV electrons to geosynchronous altitude from $x \approx -10 R_E$.

Figure 14 shows the data for two pitch angle ranges over the 1.5 day period of the MeV

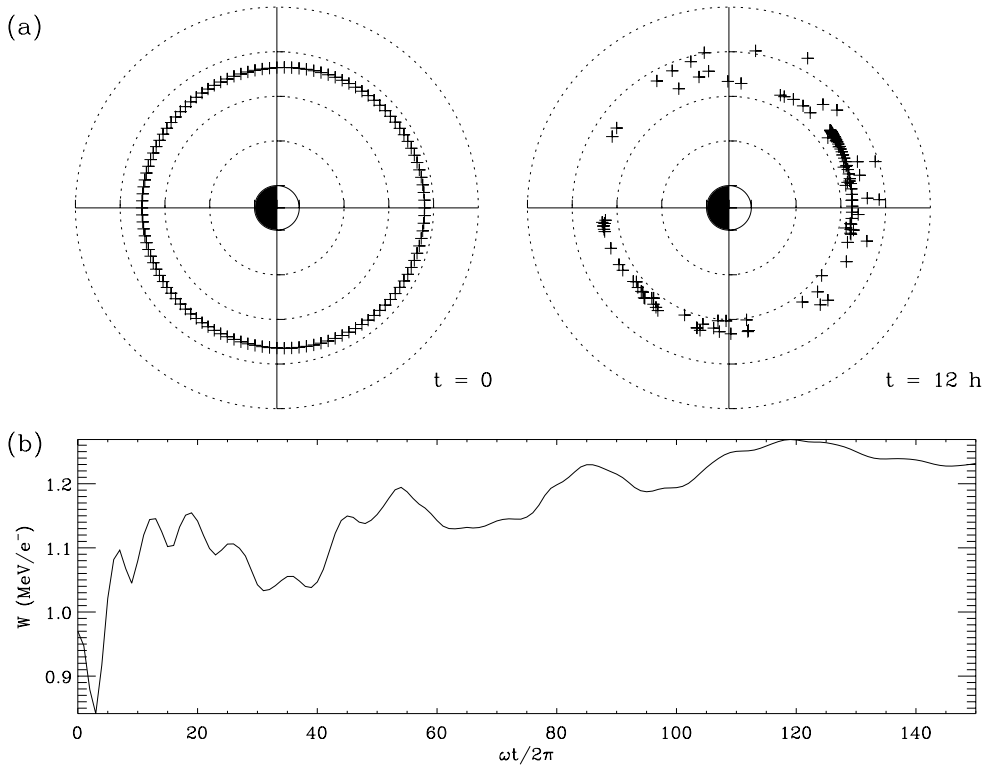

Figure 13. (a) Particle positions for a ring of near-geosynchronous particles moving in a 2 mHz, 3 mV/m toroidal oscillation with an imposed dawn-dusk convection electric field of 5 mV/m. (b) Average particle energy for particles depicted in (a), as a function of wave cycle. (from Elkington et al. (1999)).

electron population buildup (Ingraham et al., 2001). The near-perpendicular pitch angle electrons show a clear correlation with substorm activity, leading to a flux enhancement which is superimposed on a slower, more general flux increase. The tendency of the substorm electrons to form a "pancake" pitch angle distribution at the time of injection has long been recognized (Baker et al., 1978). This is the natural consequence of the electrons being transported from deeper in the tail to geosynchronous altitudes by the substorm inductive electric field while conserving μ and J, since the near-perpendicular pitch angles are energized more efficiently than the near-parallel pitch angles (Schulz and Lanzerotti, 1974).

While this clearly shows that substorms can contribute to relativistic electron buildup, the question of what supplies the mid-tail source population for this process remains unsolved.

3.7. Cusp source

Sheldon et al. (1998) presented observations of energetic electrons in the Earth's outer cusps, and speculated about possible acceleration mechanisms in the cusp. They showed that the phase space densities observed there are equal or greater than the phase space densities observed in the radiation belts at constant magnetic moment, thus allowing the possibility of diffusive filling of the radiation belts from the cusp. Fritz et al. (2000) sees the cusps as a possible major source of energetic particles for the inner magnetosphere.

3.8. Enhanced radial transport

One of the consequences of the internal acceleration mechanisms (Sections 3.3, 3.3.3, and 3.5) is

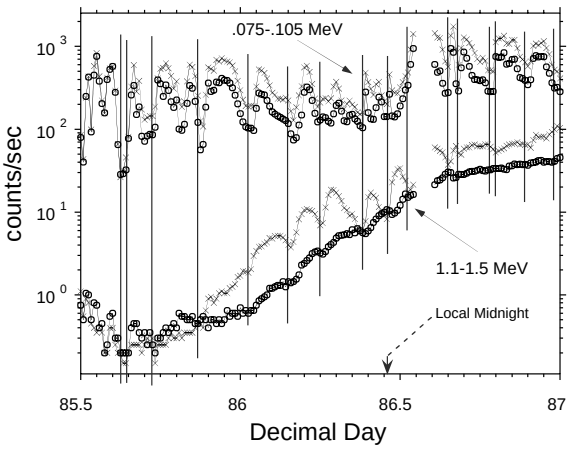

Figure 14. 12-minute average pitch angle distribution data for lower-energy (0.075–0.105 MeV) and for higher-energy (1.10–1.50 MeV) electrons from the SOPA on 1989-046. Near-parallel pitch angles (open circles), and near-perpendicular pitch angles (X's). Vertical lines indicate the times of substorm injections as determined from direct measurement, or from a dipolarization measured by a GOES magnetometer. From Ingraham et al. (2001).

a fairly localized increase of the relativistic electron phase space density (PSD). In the case of the Salammbô code simulations, the location of the increase is tied to the plasmapause location and is predicted by the code (See Figure 8). For other mechanisms the precise location is not specified and/or may be more globally distributed.

With our current spatial and instrumental coverage of the inner magnetosphere we are not able to measure the PSD globally. We need good 3-D measurements of the particle distribution function and knowledge of the local magnetic field, and often we have neither, which increases our reliance on particle and magnetic field models to "extend" our measurements; and use of magnetic field models and/or assumptions about the particle pitch angle distribution bring with them their own set of uncertainties and problems.

However, it is the slope of the PSD profiles alone that can unambiguously show the direction of diffusive transport, while maxima of the PSD indicate source locations. The question of transport from an external source versus internal acceleration could be simply answered if we knew the PSD globally in the inner magnetosphere.

Selesnick and Blake (2000) used data from the POLAR spacecraft to track the PSD during storms. POLAR yields non-equatorial cuts through the radiation belts, roughly every 10 hours. To compare these radial profiles they had to be transformed to an equatorial reference plane by use of a magnetic field model. They found that depending on the model used a wide variety of PSD profiles, including both inward and outward directions for the radial gradients, could be found.

Hilmer et al. (2000) and McAdams et al. (2001) used data from GPS at its equatorial crossing near $L = 4.2$ and LANL geosynchronous satellites near $L = 6.6$. This yields at least two points on the curve of the equatorial PSD. For all the storms examined by these authors (34) the PSD at geosynchronous ($L = 6.6$) was found to be always larger than that at GPS at the equator ($L = 4.2$). Figure 15 shows the PSD at LANL and GPS for one of the four storms examined by McAdams et al. (2001). For all four storms the gradient in phase space density is larger at smaller μ. At lower values of μ the phase space density decreases with time and the gradient remains nearly constant. At higher values of μ the phase space density increases or remains nearly constant. The increase is more rapid at $L \sim 4.2$; so the gradient decreases with time. This is consistent with the findings of Brautigam and Albert (2000), who used data from CRRES and estimated PSD profiles throughout the October 9, 1990, magnetic storm. They found that radial diffusion propagates the outer boundary variations into the heart of the outer radiation belt, accounting for both significant decreases and increases in the <1 MeV electron flux throughout that region.

Li et al. (1997b) investigated a possible solar wind source for energetic particles. In a first simple approach they compared the phase space densities in the solar wind to those at geosynchronous, under the assumption that the PSD is preserved by whatever entry mechanism takes place. They found that the solar wind would not be a sufficient source for the observed inner mag-

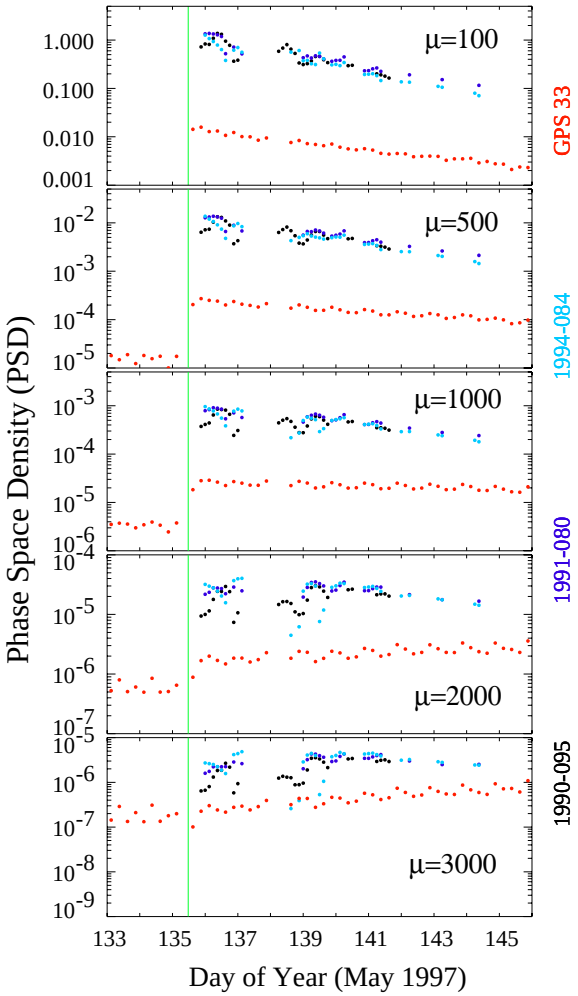

Figure 15. Phase space density (cm^{-2} s^{-1} MeV^{-2}) at constant μ at $L = 4.25 \pm 0.125$ (GPS, red) and $L = 6.6 \pm 0.125$ (LANL, blues) for different values of μ (in MeV/G). Panels show the phase space density for the two L shells at increasing values of μ for May 1997. From McAdams et al. (2001).

netospheric PSD levels.

In a more recent work Li et al. (2001) developed a model to predict MeV electrons at geostationary orbit on the basis of solar wind measurements. This model depends only on a mid-tail source and radial diffusion. The model has radial diffusion coefficients which depend on the solar wind velocity, the southward component of the interplanetary magnetic field, and on solar wind velocity fluctuations. The controlling variable is by far the solar wind velocity. The PSD at the outer boundary at L=11 assumes a fairly constant phase space density. This is probably unrealistic but does not matter much since the variation of the diffusion coefficients has a much larger effect than the variation of the source population intensity. The results of this model are shown in Figure 16 for the first half of 1995. The top panel shows the solar wind speed input featuring several repetitive high speed solar wind streams. The middle panel shows the derived radial diffusion coefficients, and the bottom panel is a comparison between the model and data fluxes at L=6.6. The prediction efficiency is 0.82 with a linear correlation of 0.85, which is quite remarkable.

The model coefficients were obtained by "training" the model on 1995 and 1996 geosynchronous data. The same static model coefficients were then used for other years, which still maintained a prediction efficiency of 0.80 over the whole 1995-1999 data period.

While this model leaves the question open of how a seed population for this process at $L = 11$ is maintained or produced, or transported into the trapping region, the model performance, at a minimum, makes a strong case that the processes are predictable (i.e. not chaotic) and are based on a low-dimensional solar wind input function.

4. Statistical work

The most exhaustive statistical study of the geosynchronous response has been performed by O'Brien et al. (2001). The authors used the extensive geosynchronous data sets available (GOES, LANL) to first establish a continuous time line of 1-hr average energetic electron fluxes mapped to a fixed noon reference point.

O'Brien et al. (2001) then performed a superposed epoch analysis to determine which parameters in the solar wind and magnetosphere have statistically significantly different characteristics for magnetic storms that do versus storms that do not generate relativistic electrons at geosynchronous, referred to as "events" and "non-events". Magnetic storms selected in this study

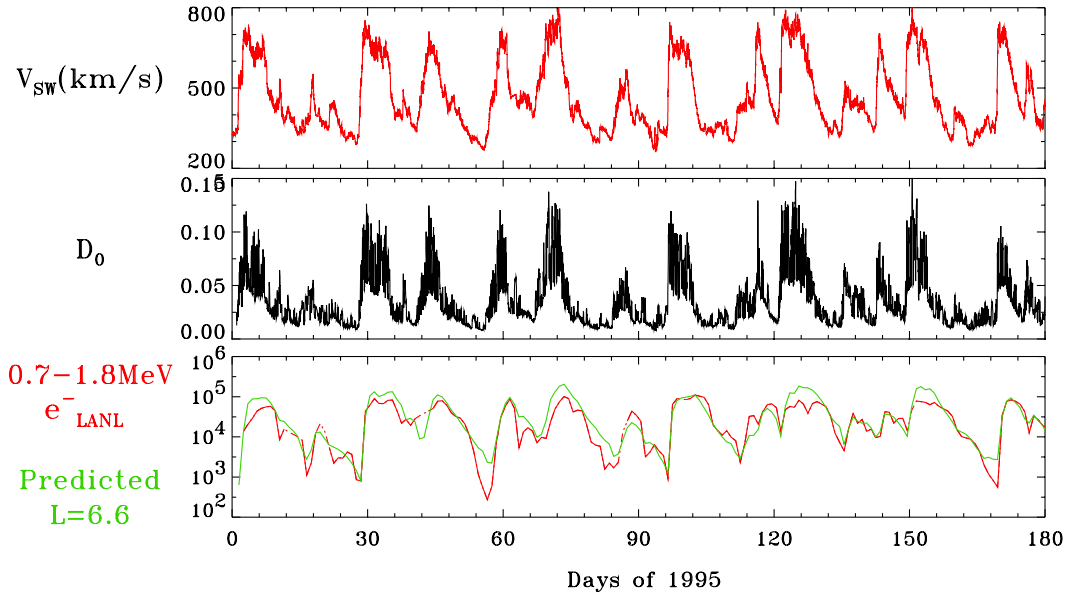

Figure 16. Most relevant solar wind and model parameters and model prediction/data comparison for geostationary relativistic electron fluxes for the first half of 1995 (from Li et al. (2001)).

are for minimum Dst < -50 nT with a moderate to low pre-storm flux. Relativistic electron "events" are defined as those which have average post-minimum Dst fluxes higher than the pre-minimum for a period 48 to 72 hours after minimum Dst; "non-events" do not have higher post-minimum Dst fluxes. The results are shown in Figure 17, in black for the events, and gray for the non-events. Panel (a) shows the two types of relativistic electron response, with the before and after responses being completely distinct after 12 hours. The lower energy electrons in panel (b) respond above prestorm in both sets, implying an energy-dependent mechanism. Panel (c) shows solar wind velocity to be higher for electron events compared to non-events almost throughout the storm. Panel (d) is the one of most interest here showing the ULF power as measured by ground stations. The event and non-event traces become most distinct 12 hours after Dst minimum: elevated ULF power in a 12 period after storm onset seems to be a good indicator of subsequent relativistic electron enhancements. The traces for AE (panel e) and Dst (panel f) are not very distinct, with slightly higher activity levels for event storms versus non-event storms. All quantities apart from the solar wind speed depicted in Figure 17 are statistically similar at minimum Dst. The solar wind result was the one noted before (Paulikas and Blake, 1979; Baker et al., 1990), yet the observed range of responses for similar solar wind velocity "inputs" has always been puzzling (Blake et al., 1997). Detailed statistical analysis of the event and non-event distributions of Figure 17 has shown that the largest statistical difference is obtained for ULF power 24 hours after minimum Dst. 80% of events that have ULF thresholds of $1000 nT^2$ or higher 24 hours after minimum DST are effective in producing relativistic electrons at geosynchronous. These statistical findings also support the observations by Baker et al. (1998b,a).

While these statistical studies might not shed light on the exact mechanism of relativistic electron buildup, they nevertheless yield some useful operational thresholds for predicting the geoeffectiveness of a given storm in producing relativistic electron buildups.

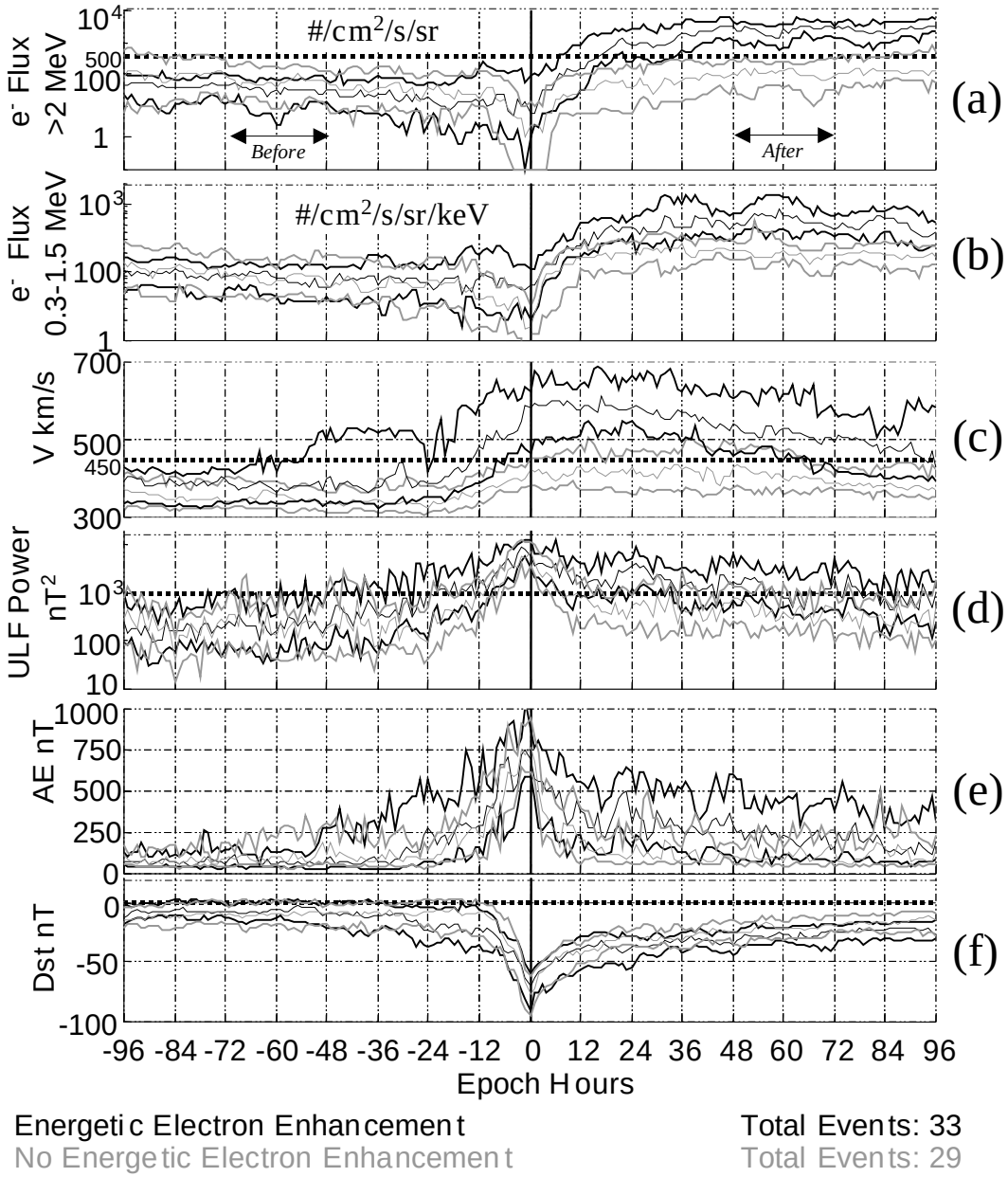

Figure 17. The evolution of quantities as a function of epoch time. Thick lines indicate upper and lower quartiles, thin lines indicate medians. Epoch zero is minimum Dst (from O'Brien et al. (2001)).

5. Relativistic electron losses

Comparatively little attention has been paid to the relativistic electron flux dropouts/losses that occur at storm onset and at other times (See Figure 4). However, a full description of the relativistic electron dynamics must include the fast loss processes that are observed. Understanding and parameterizing these losses is necessary for any comprehensive model of relativistic electron

dynamics, such as the Salammbô diffusion code.

To study the loss processes, one needs to be able to isolate them with regard to other known activity that may also lead to loss (such as magnetopause shadowing (Kistler and Larson, 2000) and the Dst effect (Kim and Chan, 1997)); this can be most easily done during moderate or small activity levels. The interesting problem here is the following: If losses are *not* caused by magnetopause shadowing or the Dst effect, then what causes them?

In Section 3.3.3 EMIC waves were identified as a possible cause of rapid pitch angle scattering which could lead to loss (Summers et al., 1998), and there is observation evidence of fast scattering into the loss cone (Lorentzen et al., 2001). It is not known if this loss is sufficient to fully explain the observations.

Onsager et al. (2001, submitted) have investigated in detail the response to a moderate (-80 nT Dst) magnetic storm (April 16, 2000). They found that the > 2 MeV electrons drop fairly abruptly but not simultaneously at different local times. Figure 18 shows the development of the flux dropout in local time using observations from two GOES and three LANL geosynchronous energetic particle detectors.

Onsager et al. (2001, submitted) argue that initially the flux dropouts are due to the development of local, tail-like magnetic field topographies, and not due to more global processes like large-scale radial diffusion. They also showed that lower energy electrons < 300 keV recover fully while the > 2 MeV electrons can be permanently lost. This indicates that in addition to the dropouts caused by tail thinning there is an energy-dependent non-adiabatic process that acted to remove these electrons from the trapping region. This had also previously been discussed by Imhof et al. (1978).

The event of Onsager et al. (2001, submitted) showed the dropout to extend in as far as $L \sim 5$. Observations by the GPS energetic particle sensors show these dropouts to be routinely observed during moderate geomagnetic activity, to L-values as low as 4.3 (T. Cayton, private communication). The example shown in Figure 4 shows the step-wise relativistic electron losses observed by GPS between $L = 4.0$ and $L = 4.5$, in response to very small storm activity (Dst ~ 30). The losses in the inner region are unrelated to the classical trapping boundary (Alfvén layer), which for these energies and activity levels is beyond the magnetopause. So what causes these losses? As Onsager et al. (2001, submitted) noted, the losses are related to stretched field topographies. There have been some suggestions that the increased field line curvature on stretched field lines could lead to the breaking of the 2nd adiabatic invariant and lead to de-trapping of the particle. While this certainly can occur for protons, can this be a process for highly relativistic electrons also? Research in this area is ongoing.

6. Summary

From the material presented in this review it becomes clear that the topic of energetic electron dynamics in the inner magnetosphere is far from being exhausted, even though energetic particle measurements and the study of charged particle motion in the Earth's magnetic field are amongst the oldest and best studied topics in our field.

With the recent advent of an increasingly dense network of observations, both spatially and temporally, the details of particle transport and acceleration have revealed ever increasing complexities. The challenge in this field remains to unravel the comparative importance of all the various mechanisms that may operate at the same time to yield relativistic electron enhancements. Many of the processes described here are certain to be active at some time during some storms - the question that remains is, "Can we establish *which* process is the most important during any given storm - and *why*?"

From the early observations or relativistic electron enhancements and their correlation with periods of high solar wind velocity and the relatively simple early recirculation models we have now proceeded to a multitude of theories and possible processes. Two classes of processes have emerged: those that rely on some kind of internal acceleration or recirculation mechanism and those that rely on increased radial transport alone. For the former, ULF waves seem to play a major role -

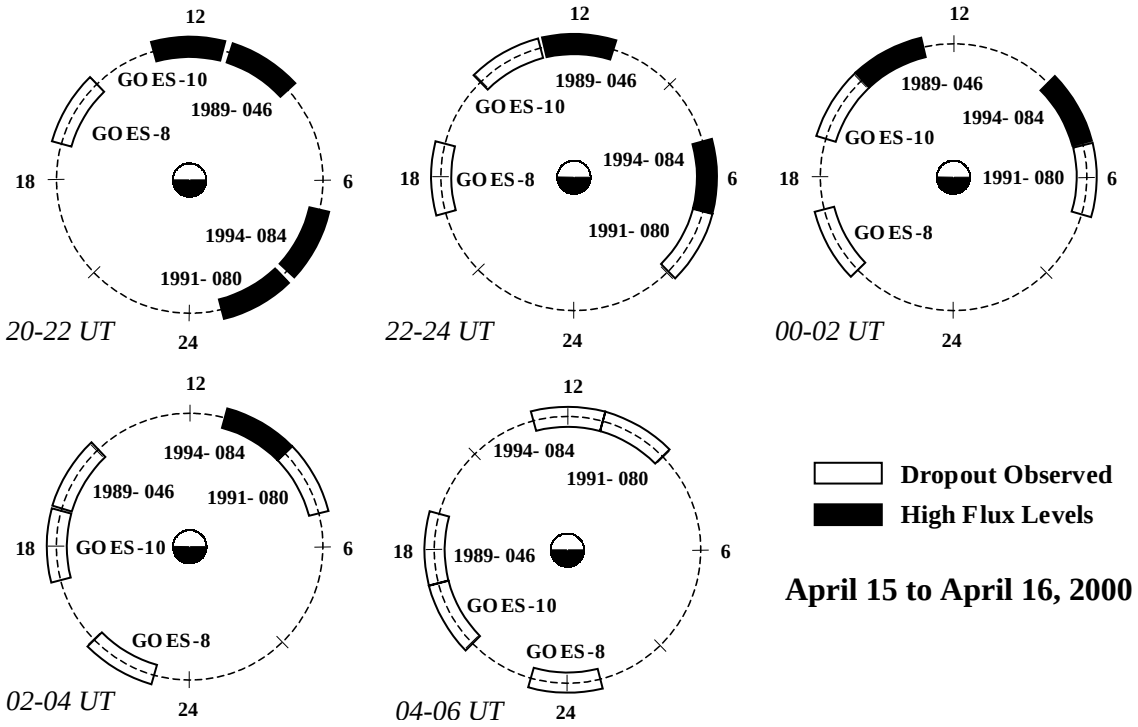

Figure 18. Development of the flux dropout over all local times. The dropout is observed first in the afternoon sector and expands to morning and eventually to local noon (Onsager et al., 2001, submitted).

both from their statistical significance in association with relativistic electron events and from the body of theoretical work that have yielded both direct and indirect mechanisms involving ULF waves that can lead to electron acceleration. For the latter, there is some evidence that a sufficient source of electrons in the mid-tail region might be all that is needed, in the presence of enhanced radial diffusion, to supply the magnetospheric fluxes that are observed at geostationary orbit. However, diffusion alone does not seem to reproduce fluxes at lower L and at $L = 6.6$. Electron energization by radial diffusion below $L = 6.6$ probably still occurs, but is no longer the most important mechanism in this region. Some or all of the other processes are probably occurring at the same time, having a significant contribution to the overall observed relativistic electron enhancements in that region.

Full investigation of either class suffers from the same experimental limitation. While we have ample data to reveal the complexity of the dynamics, we still do not have enough experimental information to enable a comprehensive study of the relative importance of the various mechanisms. To do this we need to follow the global development of the phase space density of relativistic electrons throughout the inner magnetosphere, on a time scale comparable to the acceleration and loss processes (i.e. hours). This is especially difficult during disturbed times. For this we need measurements of the particle pitch angle distribution and accurate knowledge of the magnetic field. The latter is the most critically missing ingredient here and the most enduring obstacle in this field of research. The global magnetic field structure during disturbed times is poorly modeled. This makes estimates of the relativistic particle dynamics during disturbed time little more than educated guesswork.

What is needed are high fidelity multi-point measurements of both the magnetic field and

the full particle distribution function. Currently the majority of measurements of relativistic electrons come from relatively simple environmental monitors that seldomly have direction information, on board magnetic field measurements, or both. And even given good coverage of magnetic field measurements, we do not have any magnetic field models at this time that could take advantage of this data to produce an accurate, dynamic, and global magnetic field model. Some of these constraints will be addressed by current and planned NASA missions, such as the Living With a Star program (LWS) and the Inner Magnetospheric Constellation mission currently in Sun-Earth Connection program.

References

Baker, D. N., 1996. Solar wind-magnetosphere drivers of space weather. J. Atmos. Terr. Phys. 58, 1509–1525.

Baker, D. N., Blake, J. B., Callis, L. B., Belian, R. D., Cayton, T. E., 1989. Relativistic electrons near geostationary orbit: Evidence for internal magnetospheric acceleration. Geophys. Res. Lett. 16, 559–562.

Baker, D. N., Blake, J. B., Callis, L. B., Cummings, J. R., Hovestadt, D., Kanekal, S., Klecker, B., Mewaldt, R., Zwickl, R. D., Apr. 1994. Relativistic electron acceleration and decay time scales in the inner and outer radiation belts: SAMPEX. Geophys. Res. Lett. 21, 409–412.

Baker, D. N., Blake, J. B., Klebesadel, R. W., Higbie, P. R., 1986. Highly relativistic electrons in the earth's outer magnetosphere, 1, Lifetimes and temporal history 1979–1984. J. Geophys. Res. 91, 4265–4276.

Baker, D. N., Higbie, P. R., Belian, R. D., Aiello, W. P., Hones Jr., E. W., Tech, E. R., Halbig, M. F., Payne, J. B., Robinson, R., , Kedge, S., 1988. The los alamos geostationary orbit synoptic data set. Tech. Rep. LA-8843, Los Alamos Natl. Lab., Los Alamos, N. M.

Baker, D. N., Higbie, P. R., Belian, R. D., Hones Jr., E. W., 1979. Do Jovian electrons influence the terrestrial outer radiation zone? Geophys. Res. Lett. 6, 531–534.

Baker, D. N., Higbie, P. R., Hones Jr., E. W., Belian, R. D., 1978. High-resolution energetic particle measurements at 6.6 R_E, 3, Low-energy electron anisotropies and short-term substorm predictions. J. Geophys. Res. 83, 4863–4868.

Baker, D. N., Li, X., Turner, N., Allen, J., Bargatze, L., Blake, J., Sheldon, R., Spence, H., Belian, R., Reeves, G., Kanekal, S., Jul. 1997. Recurrent geomagnetic storms and relativistic electron enhancements in the outer magnetosphere : ISTP coordinated measurements. J. Geophys. Res. 102, 14141–14148.

Baker, D. N., Mason, G. M., Figueroa, O., Colon, G., Watzin, J., Aleman, R. M., May 1993. An overview of the solar, anomalous, and magnetospheric particle explorer (SAMPEX) mission. IEEE Trans. Geosc. Remote Sens. 31, 531–541.

Baker, D. N., Mcpherron, R. L., Cayton, T. E., Klebesadel, R. W., 1990. Linear prediction filter analysis of relativistic electron properties at 6.6 R_e. J. Geophys. Res. 95, 15133–15140.

Baker, D. N., Pulkkinen, T., Li, X., Kanekal, S., Blake, B., Selesnick, R., Henderson, E., Reeves, G., Spence, H., Rostoker, G., Aug. 1998a. Coronal mass ejections, magnetic clouds, and relativistic magnetospheric electron events : ISTP. J. Geophys. Res. 103, 17279–17291.

Baker, D. N., Pulkkinen, T., Li, X., Kanekal, S., Ogilvie, K., Lepping, R., Blake, J., Callis, L., Rostoker, G., Singer, H., Aug. 1998b. A strong CME-related magnetic cloud interaction with the Earth's magnetosphere: ISTP observations of rapid relativistic electron acceleration on May 15, 1997. Geophys. Res. Lett. 25, 2975–2978.

Beutier, T., Boscher, D., Aug. 1995. A three-dimensional analysis of the electron radiation belt by the salammbô code. J. Geophys. Res. 100, 14,853–14,861.

Birn, J., Thomsen, M. F., Borovsky, J. E., Reeves, G. D., McComas, D. J., Belian, R. D., May 1998. Substorm electron injections: Geosynchronous observations and test particle simulations. J. Geophys. Res. 103, 9235–9248.

Blake, J. B., Baker, D. N., Turner, N., Ogilvie, K. W., Lepping, R. P., Apr. 1997. Correlation of changes in the outer-zone relativistic-electron population with upstream solar wind and magnetic field measurements. Geophys. Res. Lett. 24, 927–929.

Blake, J. B., Fennell, J. F., Friesen, L. M., Johnson, B. M., Kolasinski, W. A., Mabry, D. J., Osborn, J. V., Penzin, S. H., Schnauss, E. R., Spence, H. E., Baker, D. N., Belian, R., Fritz, T. A., Ford, W., Laubscher, B., Stiglich, R., Baraze, R. A., Hilsenrath, M. F., Imhof, W. L., Kilner, J. R., Mobilia, J., Voss, H. D., Korth, A., Güll, M., Fischer, K., Grande, M., Hall, D., 1995a. CEPPAD: Comprehensive energetic particle and pitch angle distribution experiment on Polar. Space Sci. Rev. 71, 531–562.

Blake, J. B., Looper, M. D., Baker, D. N., Nakamura, R., Klecker, B., Hovestadt, D., 1995b. New high temporal and spatial-resolution measurements by sampex of the precipitation of relativistic electrons. Adv. Space Res. 18, 171–186.

Blake, J. B., Selesnick, R. S., Baker, D. N., Kanekal, S., September 2001. Studies of relativistic electron injections events in 1997 and 1998. J. Geophys. Res. 106, 19157–19168.

Boscher, D., Bourdarie, S., Thorne, R. M., Abel, B., 2000. Influence of the wave characteristics on the electron radiation belt distribution. Adv. Space Res. 26 (#1), 163–166.

Bourdarie, S., Bosher, D., Beutier, T., Sauvaud, J. A., Blanc, M., Friedel, R. H. W., 1996. A physics based model of the radiation belt flux at the day timescale. In: Proceedings of the Symposium on Environment Modelling for Space-Based Applications, SP-392. ESA, ESA Publications Division, ESTEC, Noordwijk, The Netherlands, pp. 159–163.

Brautigam, D. H., Albert, J. M., Jan. 2000. Radial diffusion analysis of outer radiation belt electrons during the October 9, 1990, magnetic storm. J. Geophys. Res. 105, 291–309.

Cayton, T. E., Belian, R. D., Gary, S. P., Fritz, T. A., Baker, D. N., 1989. Energetic electron components at geosynchronous orbit. Geophys. Res. Lett. 16, 147–150.

Elkington, S. R., Hudson, M. K., Chan, A. A., 1999. Acceleration of relativistic electrons via drift-resonant interaction with toroidal-mode Pc-5 ULF oscillation. Geophys. Res. Lett. 26, 3273–3276.

Feldman, W., Aiello, W., Drake, D., Herrin, M., Jul. 1985. The BDD II: An improved electron dosimeter for the global positioning system. Tech. Rep. LA-10453-MS, Los Alamos Natl. Lab., Los Alamos, N. M.

Fritz, T. A., Chen, J. S., Sheldon, R. B., 2000. The role of the cusp as a source for magnetospheric particles: A new paradigm? Adv. Sp. Res. 25, 1445–1457.

Fujimoto, M., Nishida, A., 1990. Energization and anisotropization of energetic electrons in the Earth's radiation belt by the recirculation process. J. Geophys. Res. 95, 4265–4270.

Fung, S. F., Tan, L. C., Jul. 1998. Time correlation of low-altitude relativistic trapped electron fluxes with solar wind speeds. Geophys. Res. Lett. 25, 2361 –2364.

Hilmer, R. V., Ginet, G. P., Cayton, T. E., Oct. 2000. Enhancement of equatorial energetic electron fluxes near $L = 4.2$ as a result of high speed solar wind streams. J. Geophys. Res. 105, 23311–23322.

Horne, R. B., Thorne, R. M., 1998. Potential waves for relativistic electron scattering and stochastic acceleration during magnetic storms. Geophys. Res. Lett. 25, 3011.

Hudson, M. K., Elkington, S. R., Lyon, J. G., Goodrich, C. C., Rosenberg, T. J., 1999. Simulation of radiation belt dynamics driven by

solar wind variations. In: Burch, J. L., Carovillano, R. L., Antiochos, S. K. (Eds.), Sun-Earth Plasma Connections. Vol. 109 of Geophys. Monogr. Ser. AGU, Washington, D.C., pp. 171–182.

Hudson, M. K., Elkington, S. R., Lyon, J. G., Marchenko, V. A., Roth, I., Temerin, M., Blake, J. B., Gussenhoven, M. S., Wygant, J. R., Jul. 1997. Simulations of radiation belt formation during storm sudden commencements. J. Geophys. Res. 102, 14087–14102.

Hudson, M. K., Elkington, S. R., Lyons, J. G., Goodrich, C. C., 2000. Increase in relativistic electron flux in the inner magnetosphere: ULF wave mode structure. Adv. Sp. Res. 25, 2327–2337.

Imhof, W. L., Reagan, J. B., Gaines, E., 1978. Energy selective precipitation of inner zone electrons. J. Geophys. Res. 83, 4245–4254.

Ingraham, J. C., Cayton, T. E., Belian, R. D., Christensen, R., Friedel, R. H. W., Meier, M. M., Reeves, G. D., Tuszewski, M., 1999. March 24, 1991 geomagnetic storm: could substorms be contributing to relativistic electron flux buildup at geosynchronous altitude? (abstract). Eos Trans. AGU 80, Spring Meet. Suppl., S294.

Ingraham, J. C., Cayton, T. E., Belian, R. D., Christensen, R., Friedel, R. H. W., Meier, M. M., Reeves, G. D., Tuszewski, M., 2000. Substorm injection of relativistic electrons to geosynchronous orbit during magnetic storms: A comparison of the March 24, 1991 and March 10, 1998 storms (abstract). Eos Trans. AGU 81, Spring Meet. Suppl., S382.

Ingraham, J. C., Cayton, T. E., Belian, R. D., Christensen, R. A., Guyker, F., Meier, M. M., Reeves, G. D., Brautigam, D. H., Gussenhoven, M. S., Robinson, R. M., 1996. Multi-satellite characterization of the large energetic electron flux increase at $L = 4$–7, in the five-day period following the March 24, 1991, solar energetic particle event. In: Reeves, G. D. (Ed.), Workshop on the Earth's Trapped Particle Environment. AIP Conf. Proc 383, Woodbury, N. Y., pp. 103–108.

Ingraham, J. C., Cayton, T. E., Belian, R. D., Friedel, R. H. W., Meier, M. M., Reeves, G. D., Tuszewski, M. G., November 2001. Substorm injection of relativistic electrons to geosynchronous orbit during the great magnetic storm of March 24, 1991. J. Geophys. Res. 106, 25759–25776.

Kanekal, S. G., Baker, D. N., Blake, J. B., Klecker, B., Mason, G. M., Mewaldt, R. A., Nov. 2000. Magnetospheric relativistic electron response to magnetic cloud events of 1997. Adv. Space Res. 25 (#7/8), 1387–1392.

Kanekal, S. G., Baker, D. N., Blake, J. B., Klecker, B., Mewaldt, R. A., Mason, G. M., Nov. 1999. Magnetospheric response to magnetic cloud (coronal mass ejection) events: Relativistic electron observations from SAMPEX and Polar. J. Geophys. Res. 104, 24885–24894.

Kanekal, S. G., Baker, D. N., Li, X., Mewaldt, R. A., Cummings, J. R., Klecker, B., 1998. Jovian electrons in the earth's polar regions (abstract). Eos Trans. AGU, supplement 79, S234.

Kim, H.-J., Chan, A. A., Oct. 1997. Fully-adiabatic changes in storm-time relativistic electron fluxes. J. Geophys. Res. 102, 22107–22116.

Kistler, L. M., Larson, D. J., Nov. 2000. Testing electric and magnetic field models of the storm-time inner magnetosphere. J. Geophys. Res. 105, 25221–25231.

Knipp, D. J., Emery, B. A., Engebretson, M., Li, X., McAllister, A. H., Mukai, T., Kokubun, S., Reeves, G. D., Evans, D., Obara, T., Pi, X., Rosenberg, T., Weatherwax, A., Gc-Garg, M. G., Chun, F., Mosely, K., Codescu, M., 1998. An overview of the early November 1993 geomagnetic storm. J. Geophys. Res. 103, 26197–26220.

Korth, A., Friedel, R. H. W., Mouikis, C. G., Fennell, J. F., Wygant, J. R., Korth, H., 2000. Comprehensive particle and field observations

of magnetic storms at different local times from the CRRES spacecraft . J. Geophys. Res. 105, 18729–18740.

Li, X., Baker, D. N., Temerin, M., Cayton, T. E., Reeves, E. D. G., Christensen, R. A., Blake, J. B., Nakamura, R., Kanekal, S. G., Jul. 1997a. Multisatellite observations of the outer zone electron variation during the November 3–4, 1993, magnetic storm. J. Geophys. Res. 102, 14123–14140.

Li, X., Baker, D. N., Temerin, M., Reeves, G. D., Belian, R. D., Oct. 1998a. Simulation of dispersionless injections and drift echoes of energetic electrons associated with substorms. Geophys. Res. Lett 25, 3763–3766.

Li, X., Baker, M. T. D. N., Reeves, G. D., Larson, D., May 2001. Quantitative prediction of radiation belt electrons at geostationary orbit on the basis of solar wind measurements. Geophys. Res. Lett. 28, 1887–1890.

Li, X., Roth, I., Temerin, M., Wygant, J. R., Hudson, M. K., Blake, J. B., Nov. 1993. Simulation of the prompt energization and transport of radiation belt particles during the March 24, 1991 SSC. Geophys. Res. Lett. 20, 2423–2426.

Li, X. L., Baker, D. N., Temerin, M., Cayton, T., Reeves, G. D., Araki, T., Singer, H., Larson, D., Lin, R. P., Kanekal, S. G., Nov. 1998b. Energetic electron injections into the inner magnetosphere during the January 10–11, 1997 magnetic storm. Geophys. Res. Lett. 25, 2561–2564.

Li, X. L., Baker, D. N., Temerin, M., Cayton, T. E., Reeves, G. D., Selesnick, R. S., Blake, J. B., Lu, G., Kanekal, S. G., Singer, H., Mar. 1999. Sudden enhancements of relativistic electrons deep in the magnetosphere during May, 1997 magnetic storm. J. Geophys. Res. 104, 4467–4476.

Li, X. L., Baker, D. N., Temerin, M., Larson, D., Lin, R. P., Reeves, E. D. G., Looper, M., Kanekal, S. G., Mewaldt, R. A., Jul. 1997b. Are energetic electrons in the solar wind the source of the outer radiation belt? Geophys. Res. Lett. 24, 923–926.

Liu, W. W., Rostoker, G., Baker, D. N., 1999. Internal acceleration of relativistic electrons by large-amplitude ULF pulsations. J. Geophys. Res. 104, 17391–17407.

Lorentzen, K. R., Blake, J. B., Inan, U. S., Bortnik, J., Apr. 2001. Observations of relativistic electron microbursts in association with vlf chorus. J. Geophys. Res. 106, 6017–6027.

McAdams, K. L., Reeves, G. D., May 2001. Non-adiabatic relativistic electron response. Geophys. Res. Let 28, 1879–1882.

McAdams, K. L., Reeves, G. D., Friedel, R. H. W., Cayton, T. E., Jun. 2001. Multi-satellite comparisons of the radiation belt response to the GEM magnetic storms. J. Geophys. Res. 106, 10869–10882.

Meier, M. M., Belian, R. D., Cayton, T. E., Christensen, R. A., Garcia, B., Grace, K. M., Ingraham, J. C., Laros, J. G., Reeves, G. D., 1996. The energy spectrometer for particles (ESP): Instrument description and orbital performance. In: Reeves, G. D. (Ed.), Proceedings of the TAOS Workshop on the Earth's Trapped Particle Environment. Vol. AIP Conference Proceedings 383. Am. Inst. of Phys., Woodbury, N. Y., pp. 203–210.

Nakamura, R., Baker, D. N., Blake, J. B., Kanekal, S., Klecker, B., Hovestadt, D., 1995. Relativistic electron-precipitation enhancements near the outer edge of the radiation belt. Geophys. Res. Lett. 22, 1129–1132.

Nakamura, R., Kamei, K., Kamide, Y., N.Baker, D., Blake, J. B., Looper, M., 1998. SAMPEX observations of storm-associated electron flux variations in the outer radiation belt. J. Geophys. Res. 103, 26261–26269.

Nakamura, R., M.Isowa, Kamide, Y., Baker, D. N., Blake, J. B., Looper, M., Jul. 2000. SAMPEX observations of precipitation bursts in the outer radiation belt. J. Geophys. Res. 105, 15875–15885.

Nishida, A., 1976a. Outward diffusion of energetic particles from the Jovian radiation belt. J. Geophys. Res. 81, 1771–1773.

Nishida, A., 1976b. Outward diffusion of energetic particles from the Jovian radiation belt. J. Geophys. Res. 81, 1771–1773.

Obara, T., Den, M., Miyoshi, Y., Morioka, A., 2000a. Energetic electron variation in the outer radiation zone during early may 1998 magnetic storm. J. Atmos. Terr. Phys. 62, 1405–1412.

Obara, T., Nagatsuma, T., Den, M., Miyoshi, Y., Morioka, A., 2000b. Main-phase creation of "seed" electrons in the outer radiation belt. Earth Planets Space 52, 41–47.

Obara, T., Nagatsuma, T., Onsager, T. G., 1998. Effects of the interplanetary magnetic field (IMF) on the rapid enhancement or relativistic electrons in the outer radiation belt during the storm recovery phase. In: Kokubun, S., Kamide, Y. (Eds.), Fourth International Conferecne on Substorms. Terra/Kluwer Publications, Tokyo, pp. 215–218.

O'Brien, T. P., McPherron, R. L., Sornette, D., Reeves, G. D., Friedel, R., Singer, H. J., Aug. 2001. Which magnetic stroms produce relativistic electrons at geosynchronous orbit? J. Geophys. Res. 106, 15533–15544.

Onsager, T. G., Rostoker, G., Kim, H. J., Reeves, G. D., Obara, T., Smithtro, C., 2001, submitted. Radiation belt electron flux dropouts: Local time, radial, and particle-energy dependence. J. Geophys. Res. 106.

Paulikas, G. A., Blake, J. B., 1971. Models of the trapped radiation environment. Volume 7 - Long term time variations. Tech. rep., NASA, Washington, DC, United States.

Paulikas, G. A., Blake, J. B., May 1979. Effects of the solar wind on magnetospheric dynamics: Energetic electrons at the synchronous orbit. In: Olson, W. (Ed.), Quantitative Modeling of the Magnetospheric Processes. Vol. 21 of Geophys. Monogr. Ser. AGU, Washington D.C., pp. 180–202.

Reeves, G. D., Jun. 1998. Relativistic electrons and magnetic storms: 1992-1995. Geophys. Res. Lett. 25, 1817–1820.

Reeves, G. D., Baker, D. N., Belian, R. D., Blake, J. B., Cayton, T. E., Fennell, J. F., Friedel, R. H. W., Li, X., Meier, M. M., Selesnick, R. S., Spence, H. E., Sep. 1998. The global response of relativistic radiation belt electrons to the January 1997 magnetic cloud. Geophys. Res. Lett. 25, 3265–3268.

Roederer, J. G., 1970. Dynamics of Geomagnetically Trapped Radiation. Springer-Verlag, New York.

Rostoker, G., Skone, S., Baker, D. N., Oct. 1998. On the origin of relativistic electrons in the magnetosphere associated with some geomagnetic storms. Geophys. Res. Let 25, 3701–3704.

Roth, I., Temerin, M., Hudson, M. K., 1999. Resonant enhancement of relativistic electron fluxes during geomagnetically active periods. Ann. Geophys. 17, 631–638.

Schulz, M., Lanzerotti, L. J., 1974. Particle Diffusion in the Radiation Belts. Springer-Verlag, New York.

Selesnick, R. S., Blake, J. B., Jul. 1998. Radiation belt electron observations following the January 1997 magnetic cloud event. Geophys. Res. Lett. 25, 2553–2556.

Selesnick, R. S., Blake, J. B., Feb. 2000. On the source location of radation belt relativistic electrons. J. Geophys. Res. 105, 2607–2624.

Sentman, D. D., Allen, J. A. V., Goertz, C. K., 1975. Recirculation of energetic particles in Jupiter's magnetosphere. Geophys. Res. Lett. 2, 465.

Sheldon, R. B., Spence, H. E., Sullivan, J. D., Fritz, T. A., Chen, J., 1998. The discovery of trapped energetic electrons in the outer cusp. Geophys. Res. Lett. 25, 1825–1828.

Space Systems Loral, 1996. Space environment monitor subsystem. In: GOES I-M Databook, Revison 1. Space Systems Loral, Palo Alto, Calif., pp. 58–66.

Summers, D., Ma, C., 2000. A model for generating relativistic electrons in the earth's inner magnetosphere based on gyroresonant wave-particle interactions. J. Geophys. Res. 105, 2625–2639.

Summers, D., Thorne, R. M., Xiao, F., 1998. Relativistic theory of wave-particle resonant diffusion with application to electron acceleration in the magnetosphere. J. Geophys. Res. 103, 20487–20500.

Temerin, M., Roth, I., Hudson, M. K., Wygant, J. R., 1994. New paradigm for the transport and energization of radiation belt particles (abstract). Eos Trans. AGU 75(44), Fall Meet. Suppl., 538.

Vampola, A. L., Osborne, J. V., Johnson, B. M., 1992. CRRES magnetic electron spectrometer AFGL-701-5A (MEA). J. Spacecr. Rockets 29, 592–594.

Williams, D. J., Apr. 1966. A 27-day periodicity in outer zone trapped electron intensities. J. Geophys. Res. 71, 1815–1826.

Williams, D. J., 1987. The Earth's ring current: Present situation and future thrusts. Phys. Scr. T18, 140–151.

Zaharia, S., Cheng, C. Z., Johnson, J. R., Aug. 2000. Particle transport and energization associated with substorms. J. Geophys. Res. 105, 18741–18752.